p21-Activated Kinase 4 and Ischemic Acute Kidney Injury in Mice and Humans

Hwang Chan Yu[1], Byeoung Hoon Chung[2], Yoejin Kim[1], Yoonji Lee[3], Sangkyu Lee[4], Hong Pil Hwang[2], Hee Chul Yu[2], Kyung Pyo Kang[5], Seung-Yong Seo[6,$], Eun Ju Bae[7,$], and Byung-Hyun Park[1,$]

[1]Graduate School of Medical Science and Engineering, Korea Advanced Institute of Science and Technology, Daejon 34141, Republic of Korea

[2]Department of Surgery, Jeonbuk National University Medical School, Jeonju 54896, Republic of Korea

[3]College of Pharmacy, Chung-Ang University, Seoul 06974, Republic of Korea

[4]School of Pharmacy, Sungkyunkwan University, Suwon 16419, Republic of Korea

[5]Department of Internal Medicine, Jeonbuk National University Medical School, Jeonju 54896, Republic of Korea

[6]College of Pharmacy, Gachon University, Incheon 21936, Republic of Korea

[7]School of Pharmacy, Jeonbuk National University, Jeonju 54896, Republic of Korea

Contents

1. Supplemental Methods

Animals

Pak4$^{flox/flox}$ mice (#015828, B6.129S2-*Pak4*$^{tm2.1Amin}$/J) and *Ggt1-Cre* mice (#012841, *Tg(Ggt1-Cre)M3Egn/J*) were obtained from the Jackson Laboratory (Bar Harbor, ME, USA) and crossed to generate proximal tubule-specific *Pak4* knockout mice (*Pak4*$^{flox/flox}$;*Ggt1-Cre*). All mice were backcrossed to the C57BL/6J strain for at least six generations, and the heterozygous offspring were intercrossed, producing beige mice. For genotyping, tail tips were incubated with STE buffer (0.2% SDS, 100 mM Tris, 5 mM EDTA, and 200 mM NaCl, pH 7.4) and 0.5 mg/ml proteinase K for 12 h at 56°C after which they were subjected to a two-step PCR with specific forward (5′-GATGCAACGAGTGATGAG-3′) and reverse (5′-TCGGCTATACGTAACAGG-3′) primers. Amplification of a 496-bp band confirmed the *Pak4* genotype. *Pak4* KO mice and WT littermates (*Pak4*$^{flox/flox}$) were fed a standard laboratory normal chow diet. Food intake and body weight were monitored every week throughout the experiments. All experimental mice were housed in a controlled barrier facility (12 h light/dark cycle, 22±1°C, 60−70% humidity). This study protocol was approved by the Institutional Animal Care and Use Committee of Jeonbuk National University Hospital (Permit No: JBUH-2021-14).

Patients and biopsy material

Human renal tissue was procured during kidney transplantations conducted at the Surgery department of Jeonbuk National University Hospital (Jeonju, Korea), spanning from March 2022 to January 2024. Among the 15 human renal tissues collected, 8 were from living donors

and 7 were from deceased donors. Punch needle core biopsies were acquired from all transplanted kidneys at two distinct time points: 1) before reperfusion, following nephrectomy, flushing with ice-cold Histidine-Tryptophan-Ketoglutarate solution (Custodiol®), and storage, but prior to implantation, and 2) after reperfusion, approximately 20 to 40 min post-kidney reperfusion, just before wound closure. All biopsies were promptly frozen in liquid nitrogen and stored at −80°C. Detailed information regarding crucial clinical parameters and outcome indicators is provided in Supplemental Table 3. Noteworthy, no significant differences were observed between living and deceased donor renal allografts in terms of donor age, HLA-A, -B, and -DR mismatches, the number of retransplants, anastomosis time, and recipient sex. All patients granted written informed consent, and the study received approval from the Institutional Review Board of Jeonbuk National University Hospital (Permit No: JBUH 2022-02-029).

Induction of AKI

Renal I/R was conducted using eight-week-old male mice that were anaesthetized with a xylazine hydrochloride (25 mg/ml, i.p.) as described previously with slight modification [1]. In the I/R group, both renal pedicles were clamped through midline abdominal incision for 25 min using a non-traumatic microvascular clip and then subjected to reperfusion for various time points. In addition, another group of mice was only subjected to the midline abdominal incision (sham-operated control group). The body temperature was controlled at 36.8–37.2° C during surgery with a temperature-controlled operating table. Blood samples were taken for renal function assessment and kidneys were collected for histopathology, Western blot, and qPCR analyses.

To establish a cisplatin-induced AKI model, eight-week-old WT and *Pak4* KO mice were administered cisplatin (0.5 mg/kg) intraperitoneally. The mice were sacrificed 2.5 days post-

injection.

Biochemical analysis

Blood urea nitrogen (BUN, #K024-H1), creatinine (#K002-H1, both from Arbor Assays, Ann Arbor, MI, USA), TNF-α (#BMS607-3), IL-6 (#KHC-0061, both from Invitrogen, Carlsbad, CA, USA), IL-1β (eBioscience, San Diego, CA, USA), CCL2 (Peprotech, Rocky Hill, NJ, USA), TG (#80-INSMS-E01, ALPCO, Salem, NH, USA), caspase-3 assay kit (#G8090, Promega,), caspase-9 assay kit (#G8210, both from Promega, Madison, WI, USA), MDA (#ab118970), GSH (#ab235670), GSSG (#ab65322), GPx3 (#ab256470), and GPx activity (#ab102530, all from Abcam, Cambridge, UK) were measured using specific kits following the manufacturer's instructions.

Histological analysis

The kidneys were collected and fixed with 10% formalin at room temperature for 24 h and were then paraffin-embedded. Tissues were cut into 5-μm thick sections, which were stained with hematoxylin and eosin (H&E) at room temperature for light microscopy. Histopathological damage was defined as tubular necrosis, loss of brush border, cast formation, and tubular dilatation [2]. The degree of tubular injury was estimated at a ×200 magnification using 10 randomly selected fields for each kidney according to the following standard: 0, normal; 1, damage involving <10% of tubules; 2, damage involving 10–25% of tubules; 3, damage involving 26–45% of tubules; 4, damage involving 46–75% of tubules; 5, damage involving 75–100% of tubules. Tubular necrosis was quantitated as the percentage of tubules in the outer medulla in which epithelial necrosis or necrotic debris was observed in H&E-stained sections. Tissue iron detection was performed using a Prussian blue staining kit

(#ab150674, Abcam).

Immunohistochemistry

Kidney tissues were immediately placed in fixative (10% formalin solution in 0.1 M PBS). Immunohistochemical staining was performed using the DAKO Envision system (DAKO, Carpinteria, CA, USA). After deparaffinization and hydration, tissue sections (5 μm) were stained with primary antibodies against PAK4 (#sc390507, Santa Cruz Biochemicals, Dallas, TX, USA), F4/80 (#ab6640), podocin (#PA1322-1, Boster Bio, Pleasanton, CA, USA), aquaporin 4 (#ab259318), *Lotus tetragonolobus* lectin (#ab190834), Plin2 (#ab1083230), or CD11b (#ab 128797, all from Abcam) at 4°C overnight. After washing with PBS, secondary antibodies (#A11001, Alexa Fluor 488-conjugated goat anti-mouse IgG1 or #A11012, Alexa Fluor 594-conjugated goat anti-rabbit IgM, both from Thermo Fisher Scientific, Waltham, MA, USA) were incubated for 1 h at 37°C. Sections were then counterstained with 4′,6-diamidino-2-phenylindole (DAPI). Slides were photographed under a Zen blue microscope (Carl Zeiss, Oberkochen, Germany). Quantifications of intensity, area stained, and cell numbers were performed using ImageJ 1.52p software (National Institutes of Health, Bethesda, MD, USA).

TUNEL assay

Apoptotic cells were detected using a TUNEL assay kit (#G3250, Promega). After treatment with a nucleotide mix and terminal deoxynucleotide transferase (rTdT), tissue sections were incubated at 37°C for 1 h. Apoptotic cells, counterstained with hematoxylin, were counted under a microscope (×400) and expressed as the apoptosis index (number of apoptotic bodies/100 cells).

Subcellular fractionation, Western blotting, and co-immunoprecipitation (Co-IP)

Tissue homogenates or cell lysates (20 μg) were separated by 7–12% SDS-PAGE and transferred to PVDF membranes. After blocking with 5% skim milk, blots were probed with primary antibodies against specific antibodies (Supplemental Table 4). For co-immunoprecipitations, 500 μg protein was incubated with anti-PAK4 (#G222) or nonspecific IgG (#2729, both from Cell Signaling Technology, Danvers, MA, USA) overnight at 4°C followed by protein G agarose (#15920-010, Invitrogen) for 2 h at 4°C. Blots were probed with antibodies against calreticulin (#92635), HSP60 (#4870, both from Cell Signaling Technology), spectrin (#ab154811, Abcam), or GPx3 (#ab256470, both from Abcam).

Signals were detected with horseradish peroxidase (HRP)-conjugated goat anti-mouse (#11001), goat anti-rat (#11012, both from Thermo Fisher Scientific), or goat anti-rabbit IgG (#2729, Cell Signaling Technology). Immunoreactive bands were detected with a Las-4000 imager (GE Healthcare Life Science, Pittsburgh, PA, USA).

RNA isolation, qPCR and genotyping

Total RNA was extracted from frozen kidney tissues or HK-2 cells using TRIzol reagent (Invitrogen). RNA was precipitated with isopropanol, dried using 70% ethanol, and dissolved in diethyl pyrocarbonate-treated distilled water. First-strand cDNA was generated using the random hexamer primer provided in the first-strand cDNA synthesis kit (Applied Biosystems, Foster City, CA, USA). Specific primers were designed using PrimerBank (https://pga.mgh.harvard.edu/primerbank, Supplemental Table 5). qPCR reactions were performed in a final volume of 10 μl containing 10 ng reverse-transcribed total RNA, 200 nM forward and reverse primers, and PCR master mixture. qPCR was performed in 384-well plates using an ABI Prism™ 7900HT Sequence Detection System (Applied Biosystems).

Isolation of renal tubular cells, cell culture and transient transfection

Renal cortical tissues were isolated from three-week-old male C57BL/6J mice and treated with 0.1% type II collagenase (Gibco, Grand Island, NY, USA) at in a 5% CO_2 incubator for 60 min. Following incubation, the supernatant was filtered through two cell strainers with pore sizes of 200 μm and 85 μm (pluriSelect Life Science, Leipzig, Germany). The primary tubule fragments were then resuspended in DMEM/F12 medium supplemented with 1% heat-inactivated FBS, 15 mM HEPES, 50 nM hydrocortisone, insulin/transferrin/selenium (10 ml/l), nonessential amino acids, penicillin (100 units/ml), and streptomycin (100 mg/ml). The collected tubule fragments were centrifuged at 170 × g for 5 min, seeded onto collagen-coated 100 mm dishes, and incubated for 7 days with the medium replaced every 2 days. After reaching confluency, the primary tubular cells were split and reseeded onto collagen-coated 60 mm dishes at a density of 6×10^5 cells per plate.

The human embryonic kidney 293T fibroblasts (HEK293T, #CRL-3216) and human proximal tubular cells (HK-2, #CRL-2190) were obtained from the American Type Culture Collection (Manassas, VA, USA). Culture media were supplemented with penicillin (100 units/ml) and streptomycin (100 mg/ml). Both cell lines were cultured in DMEM containing 10% FBS. Cells were maintained at 37°C in a humidified environment with 5% CO_2. For glutathione peroxidase 3 transcriptional activity assays, the HK-2 cells with or without PAK4 silencing were seeded in 12-well plates. Twenty-four-hour post seeding, cells were transfected with 1 μg of a plasmid containing a promoter (-1.4 kb to TSS) driving luciferase expression and exposed to hypoxia−reoxygenation (H/R). Luminescence was measured using glutathione peroxidase 3 reporter gene assay (#MPRM39605, GeneCopoeia, Rockville, MD, USA).

Hypoxia−reoxygenation protocol

HK-2 or primary renal tubular cells were incubated at 37°C in anaerobic chamber (MYTEMPmini digital incubator, H2200-HC, Benchmark, Sayreville, USA) with oxygen-absorbing packs (AnaeroGen, Oxoid, Basingstoke, United Kingdom). This method has been shown to achieve oxygen levels in the jar below 1%. Following 25 min of hypoxia, reoxygenation of cells was initiated by opening the chamber and replacing the hypoxic medium with oxygenated medium.

Chromatin immunoprecipitation (ChiP) assay

HK-2 cells were chopped and cross-linked by incubating cells in 1% formaldehyde for 15 min at room temperature. The cross-linking process was halted by a 3 minute-incubation with 100 mM glycine (pH 7.0). Subsequently, the ChIP assay was performed using ChIP Enzymatic Chromatin IP Kits (Cell Signaling Technology). Chromatins were immunoprecipitated overnight at 4°C with antibodies to SP1 (#sc17824, Santa Cruz Biochemicals), PPARγ (#2430), or nonspecific IgG (#2729, both from Cell Signaling Technology). qPCR for the ChIP DNA was performed to determine the interaction of either SP1 or PPARγ with the proximal region of the *Gpx3* promoter. Data were normalized to the input.

Proximity ligation assay (PLA)

Protein interactions were assessed using a Duolink PLA kit (#DUO92002, Sigma-Aldrich, St. Louis, MO, USA) as previously described [3]. Briefly, HK-2 cells or renal tissues were fixed with 10% neutral buffered formalin, permeabilized with PBS/0.1% Triton X-100, and then incubated with the following antibody pairs: anti-PAK4 (#sc-390507, Santa Cruz Biochemicals)

in conjunction with either anti-GPx3 (#ab256470) or anti-GPx4 (#ab41787, both from Abcam). Samples were then incubated with Duolink *in situ* PLA Probes (anti-rabbit Minus and anti-mouse Plus) for 1 h. Signals were amplified with polymerase using *in situ* Detection Reagents Green. Finally, cells or tissues were counterstained with DAPI and images were captured using an LSM880 confocal laser scanning microscope (Carl Zeiss, Oberkochen, Germany).

Phosphoproteome analysis

Kidney cortex samples (100 mg) from *Pak4* KO mice and their littermates following I/R injury were conducted in phosphoproteome analysis. The primary screening was performed based on the difference in total phosphorylation levels between the two genotypes. Based on the adjusted phospho-ratio (WT/KO>2), the top six proteins with the highest scores were selected and identified by LC-MS/MS after in-gel digestion of the protein spots of interest. Potential proteins of interest were defined as phospho-tryptic peptides that exhibited 1) a negative or positive change of >2-fold in the phosphorylation state (phosphoprotein/protein) and 2) a change with a $p<0.05$ across the three replicates.

LC-MS/MS and peak alignment

The phosphopeptide was analyzed with a Q-Exactive HF-X mass spectrometer (Orbitrap MS, Thermo Fisher Scientific) connected to UHPLC system (Ultimate 3000, Thermo Fisher Scientific) to acquire MS/MS spectra. The peptide samples were loaded into the trap column and separated on an analytical column (PepMap RSLC, 3 μm, 100Å, 75 μm × 50 cm). Each sample (2 μl) was injected onto a binary mobile phase consisting of water in 0.1% formic acid as mobile phase A and acetonitrile in 0.1% FA as mobile phase B. A linear gradient consisting of 5–30% mobile phase B at a flow rate of 300 nl/min was employed for 60 min. Full scan and

PRM settings were as follows: spray voltage on positive mode 1.8 kV, capillary temperature 275°C, normalized collision energy 28%, max injection time 100 ms. PRM resolution was 30,000, target value 3×10^6, max injection time 64 ms, and window 0.7 m/z for precursor isolation. Mass spectra were acquired in full scan mode followed with PRM analysis between 450 and 1000 with a mass resolution of 120,000. Lock mass ion was applied as 445.12002 m/z from polydimethylcyclosiloxane for internal calibration.

MS/MS spectra for phosphopeptide identification and its site was obtained in Mascot server (version 2.8.0.1). The resulting data was queried using a FASTA containing sequence (YGALTIDGEEYIPFK) of glutathione peroxidase 3 downloaded from UniProtKB (Accession ID: P22352). Search parameters were described as follows: enzyme set as none, phosphorylation (Ser/Thr) as variable modifications. The search results were filtered with a significant threshold *p* less than 0.05. Peptide mass tolerance was set to ± 0.02 Da and fragment mass tolerance was ± 10 ppm.

In vitro kinase assay

Recombinant glutathione peroxidase 3 (1 μg, #TP720117, Origene, Rockville, MD, USA) was incubated with recombinant PAK4 (0.3 μg, #ab96405, Abcam) in assay buffer (50 mM Tris-HCl, 10 mM $MgCl_2$, 2 mM DTT and 0.1 mM EDTA, pH 7.6) containing 5 μCi of [γ-^{32}P]ATP at 30°C for 30 min. Reaction mixtures were then subjected to SDS-PAGE, and ^{32}P-labelled proteins were detected by autoradiography. For Coomassie blue staining, gel was stained in Coomassie protein stain buffer (#ab119211, Abcam) for 1 h. For peptide competition assay, synthetic 15-residue oligopeptides corresponding to each region comprising T47 (P1: IYEYGALTIDGEEYI), S165 (P2: PTSELLGTSDRLFWE) or negative control (P0: LLLAGFVSQSRGQEK) were used.

Mutagenesis of glutathione peroxidase 3

Human glutathione peroxidase 3 plasmid vector (#EX-M0197-M09, GeneCopoeia) was provided from GenScript (Tokyo, Japan). The mutants of glutathione peroxidase 3 were generated by site-directed mutagenesis (Cosmo Genetech, Seoul, Korea). $GPx3^{T47A}$, $GPx3^{T47D}$, and $GPx3^{T165A}$ mutants were generated by introducing a point mutation of the threonine residue in glutathione peroxidase 3 to alanine or aspartic acid as follows: $GPx3^{T47A}$ (ACC → GCC), $GPx3^{T47D}$ (ACC → GAC), and $GPx3^{T165A}$ (TAC → GAC).

Preparation of recombinant adeno-associated viruses (AAVs)

The AAV2-$GPx3^{WT}$ and AAV2-$GPx3^{T47A}$, containing the coding gene sequence located between two flox sites in an inverted direction with the *Ggt1-Cre* recombinase-bound moiety, were used to drive the expression of WT or mutant glutathione peroxidase 3 in the *Pak4* KO renal tubular cells. An AAV2-eGFP was used as a control. To generate AAV2-$GPx3^{WT}$, AAV2-$GPx3^{T47A}$, and $AAV2^{eGFP}$, cDNA fragments encoding inversely-ordered GPx3, $GPx3^{T47A}$, and eGFP were separately cloned into an AAV2 Inverted Terminal Repeat (VectorBuilder, Chicago, IL, USA) harboring *Ggt1-Cre* recombinase bound moieties, respectively. The AAV2 vectors were then packaged in HEK293T cells with helper vectors (E4) and AAV8:Rep-cap (VectorBuilder) vectors, in a 1:1:3 ratio. Transfection was performed using branched polyethylenimine (PEI, Sigma-Aldrich, 1:3 μg DNA to μg PEI ratio). After 72 h, cells and supernatants were separated by centrifuge in 1000 × g. Cells were placed on ice, lysed, and sonicated four times with a 1-sec pulse to obtain a cleared supernatant. Supernatants were precipitated at 4°C overnight by adding 500 mM NaCl and 40% PEG 8000 solution (Sigma-Aldrich). Purified AAV2 were washed in washing buffer and then eluted using gravity column

in AAV-pro purification kit (#6232, Takara Bio, Shiga, Japan). The purity of AAV2, exceeding 90%, was confirmed by SDS-PAGE. All AAV2s were aliquoted and stored at -80°C for further study.

For renal tubular cell-specific delivery of glutathione peroxidase 3, eight-week-old male *Ggt1-Cre* mice were randomly subjected to an intravenous injection of either AAV2^{eGFP}, AAV2-GPx3^{WT}, or AAV2-GPx3^{T47A} (1×10^{12} viral particles per mouse). One weeks after injection, the expression level of eGFP in various tissues was confirmed by qPCR to determine efficacy of AAV2 delivery.

Prediction of PAK4- glutathione peroxidase 3 complex model

Computational simulation was conducted to predict the complex model of PAK4 and glutathione peroxidase 3. The protein 3D structure of human PAK4 (PDB id: 4XBR) [4] was retrieved from the Protein Data Bank (https://www.rcsb.org). By using the FlexPepDock protocol in Rosetta [5,6], the plausible conformations of the 15-mer peptide (^{479}QRSGSSTPQRSCSAA^{493}) of glutathione peroxidase 3 were modeled at the substrate binding site of PAK4. During the simulation, the number of high-resolution structures was set to 300. Among the top-scoring ten models, the most appropriate model was manually inspected and selected. The molecular graphic figure was generated by PyMOL software (version 2.5.4, Schrödinger, New York, NY, USA).

Synthesis of PAK4 PROTAC SJ-05

All starting materials and reagents were obtained from commercial sources and used without further purification. Solvents were purified with drying cartridges through a solvent delivery system. Air- and moisture-sensitive reactions were performed under nitrogen. Flash

column chromatography was performed using silica gel 60 (230−400 mesh, Merck) with the indicated solvents. ^{1}H and ^{13}C NMR spectra were recorded using Bruker 600 MHz spectrometer. Chemical shifts are expressed in parts per million (ppm, δ) downfield from tetramethylsilane and ^{1}H NMR data were reported in the order of chemical shift, multiplicity (s, singlet; d, doublet; t, triplet; q, quartet; m, multiplet and/or multiplet resonances), coupling constant (J value) in hertz (Hz), and number of protons.

2-(4-((1-(*tert*-Butoxycarbonyl)piperidin-4-yl)methyl)piperazin-1-yl)-5-nitrobenzoic acid (1). To a solution of the *tert*-butyl 4-(piperazin-1-ylmethyl)piperidine-1-carboxylate (4.6 g, 16 mmol) and 2-fluoro-5-nitrobenzoic acid (3.6 g, 20 mmol) in THF (250 ml) was added iPr_2NEt (8.5 mL, 49 mmol). After stirring for 2 h at room temperature, the reaction mixture was poured into water and extracted with EtOAc. The combined organic layer was dried over $MgSO_4$ and concentrated *in vacuo*. The residue was purified by flash column chromatography (CH_2Cl_2/MeOH = 10:1) to afford **1** (9.50 g, 97%). ^{1}H NMR (600 MHz, CD_3OD) δ 8.34 (d, J = 2.8 Hz, 1H), 8.13 (dd, J = 9.1, 2.8 Hz, 1H), 7.09 (d, J = 9.1 Hz, 1H), 4.10 (d, J = 13.2 Hz, 2H), 3.47 (s, 4H), 3.11 (s, 3H), 2.78 (s, 4H), 1.98 (s, 1H), 1.80 (m, 2H), 1.46 (s, 10H), 1.16 (m, 2H). HRMS (FAB+) calcd for $C_{22}H_{32}N_4O_6$ $[M + H]^+$ = 449.2400, found = 449.2401.

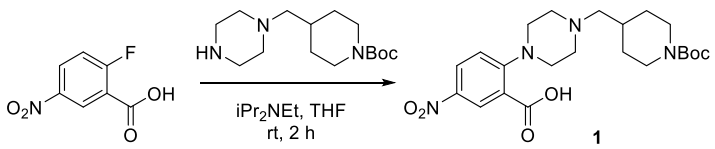

***tert*-Butyl (*R*)-4-((4-(2-(3-((2-chloro-7-((2-(trimethylsilyl)ethoxy)methyl)-7*H*-pyrrolo[2,3-**

d]py-ramidin-4-yl)amino)piperidine-1-carbonyl)-4-nitrophenyl)piperazin-1-yl)methyl)piperidine-1-carboxylate (2). To a solution of **1** (1.6 g, 3.6 mmol) and (*R*)-2-chloro-*N*-(piperidin-3-yl)-7-((2-(trimethylsilyl)ethoxy)methyl)-7*H*-pyrrolo[2,3-d]pyrimidin-4-amine (1.8 g, 3.6 mmol) in DMF (35 ml) was added EDCI (2.0 g, 11 mmol), iPr_2NEt (3.1 ml, 18 mmol) and DMAP (44 mg, 0.36 mmol). After stirring for 24 h at room temperature, the reaction mixture was poured into water and extracted with EtOAc. The combined organic layer was dried over $MgSO_4$ and concentrated *in vacuo*. The residue was purified by flash column chromatography (EtOAc/*n*-hexane = 1:1) to afford **2** (1.7 g, 59%). ^1H NMR (600 MHz, CD_3OD) δ 7.92 (dd, *J* = 9.1, 2.8 Hz, 1H), 7.46 (d, *J* = 2.7 Hz, 1H), 7.07 (dd, *J* = 19.0, 6.3 Hz, 2H), 6.66 (dd, *J* = 11.5, 3.6 Hz, 1H), 5.55–5.46 (m, 2H), 5.25 (d, *J* = 11.0 Hz, 1H), 4.42 (d, *J* = 12.6 Hz, 1H), 4.05 (d, *J* = 12.5 Hz, 3H), 3.96 (s, 1H), 3.63–3.44 (m, 3H), 3.26–3.12 (m, 4H), 2.76 (s, 1H), 2.29 (d, *J* = 7.2 Hz, 2H), 2.10 (d, *J* = 9.7 Hz, 1H), 1.79 (s, 4H), 1.45 (m, 13H), 1.09 (dd, *J* = 18.3, 5.9 Hz, 3H), 0.91–0.83 (m, 2H), -0.07 (d, *J* = 3.3 Hz, 9H). HRMS (FAB+) calcd for $C_{39}H_{58}ClN_9O_6Si$ $[M + H]^+$ = 812.4046, found = 812.4039.

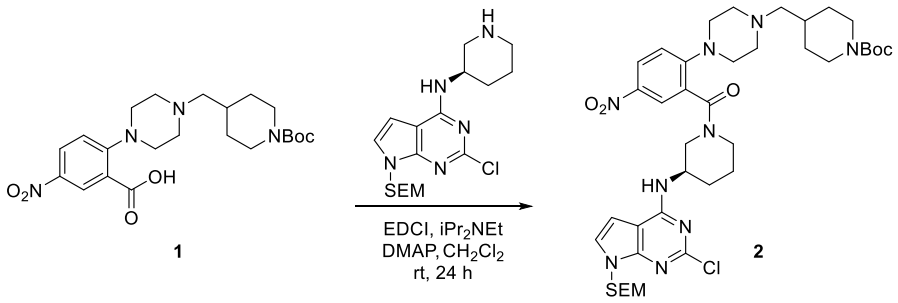

***tert*-Butyl (*R*)-4-((4-(4-amino-2-(3-((2-chloro-7-((2-(trimethylsilyl)ethoxy)methyl)-7*H*-pyrrolo-[2,3-d]pyrimidin-4-yl)amino)piperidine-1-carbonyl)phenyl)piperazin-1-yl)methyl)piperidine-1-carboxylate (3).** To a solution of **2** (0.80 g, 0.98 mmol) and 5% Pd/C (0.42 g, 20 mol%) in MeOH (10 ml) were placed under an atmosphere of H_2. After stirring for 2 h at room temperature, the reaction mixture was filtered through a Celite pad. After the filtrate

was concentrated *in vacuo* to afford **3** (0.61 g, 91%). The residue was used in the next step without further purification. HRMS (FAB+) calcd for $C_{39}H_{60}ClN_9O_4Si$ $[M + H]^+$ = 782.4304, found = 782.4308

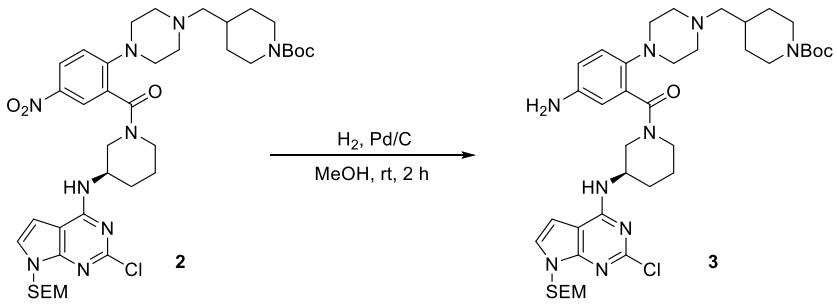

***tert*-Butyl 4-((4-((3^3*R*)-4-oxo-1^7-((2-(trimethylsilyl)ethoxy)methyl)-1^7*H*-2,6-diaza-1(4,2)-pyrrolo[2,3-d]pyrimidina-3(3,1)-piperidina-5(1,3)-benzenacyclohexaphane-5^6-yl)piperazin-1-yl)methyl)piperidine-1-carboxylate (4).** To a solution of **3** (0.32 g, 0.41 mmol), $Pd(dba)_3$ (93 mg, 25% mol), Xantphos (0.18 mg, 0.30 mmol) and NaO*t*-Bu (0.20 g, 2.0 mmol) in 1,4-dioxnae (12 ml). After stirring for 12 h at 100°C, the reaction mixture was poured into water and extracted with EtOAc. The combined organic layer was dried over $MgSO_4$ and concentrated *in vacuo*. The residue was purified by flash column chromatography (acetone/*n*-hexane = 2:3) to afford **4** (0.15 g, 50%). ^{1}H NMR (600 MHz, CD_3OD) δ 8.49 (d, *J* = 2.5 Hz, 1H), 7.23 (dd, *J* = 8.6, 2.5 Hz, 1H), 7.17 (d, *J* = 8.6 Hz, 1H), 7.02 (d, *J* = 3.6 Hz, 1H), 5.51 (s, 2H), 4.75 (d, *J* = 12.8 Hz, 1H), 4.57 – 4.50 (m, 1H), 4.12 (d, *J* = 13.4 Hz, 2H), 3.93 (s, 2H), 3.67–3.53 (m, 5H), 3.12 (d, *J* = 6.9 Hz, 4H), 3.02 (d, *J* = 12.0 Hz, 1H), 2.88–2.72 (m, 3H), 2.71–2.58 (m, 1H), 2.21 (m, 1H), 2.10 (m, 1H), 2.01 (m, 1H), 1.94–1.83 (m, 2H), 1.79 (m, 2H), 1.46 (s, 9H), 1.24–1.17 (m, 2H), 0.93–0.87 (m, 3H), -0.04 (s, 9H). HRMS (FAB+) calcd for $C_{39}H_{59}N_9O_4Si$ $[M + H]^+$ = 746.4537, found = 746.4538.

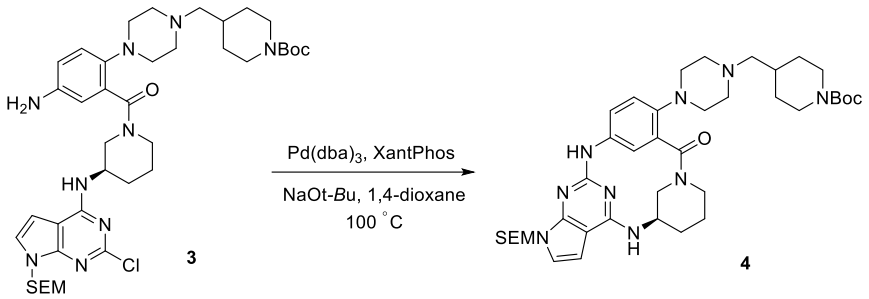

(3^3*R*)-^{5}6-(4-(Piperidin-4-ylmethyl)piperazin-1-yl)-1^7*H*-2,6-diaza-1(4,2)-pyrrolo[2,3-d]pyrimidina-3(3,1)-piperidina-5(1,3)-benzenacyclohexaphan-4-one (5). To a solution of **4** (0.15 g, 0.20 mmol) in CH_2Cl_2 (2 ml) was added TFA (2 ml) at 0°C. After stirring for 2 h, the reaction mixture concentrated *in vacuo* to afford the **5** (150 mg, 99%). ^{1}H NMR (600 MHz, CD_3OD) δ 8.56 (d, *J* = 2.5 Hz, 1H), 7.38–7.19 (m, 3H), 7.09 (d, *J* = 3.6 Hz, 1H), 6.64 (d, *J* = 3.6 Hz, 1H), 5.62 (d, *J* = 2.2 Hz, 2H), 4.83 (d, *J* = 12.6 Hz, 1H), 4.64–4.57 (m, 1H), 4.03 (dd, *J* = 14.7, 7.2 Hz, 2H), 3.73 (s, 1H), 3.54 (d, *J* = 12.9 Hz, 3H), 3.26 (d, *J* = 7.1 Hz, 3H), 3.13 (t, *J* = 12.9 Hz, 3H), 2.92–2.80 (m, 1H), 2.71 (s, 1H), 2.40–2.26 (m, 2H), 2.18 – 2.07 (m, 4H), 1.95 (m, 2H), 1.61 (m, 3H). HRMS (FAB+) calcd for $C_{28}H_{37}N_9O$ $[M + H]^+$ = 516.3199, found = 516.3200.

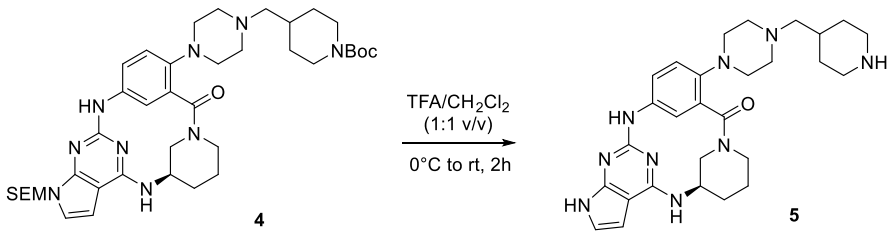

2-(2,6-Dioxopiperidin-3-yl)-5-fluoro-6-(4-((4-((3^3*R*)-4-oxo-1^7*H*-2,6-diaza-1(4,2)-pyrrolo[2,3-d]pyrimidina-3(3,1)-piperidina-5(1,3)-benzenacyclohexaphane-5^6-yl)piperazin-1-yl)methyl)piperidin-1-yl)isoindoline-1,3-dione (SJ-05). To a solution of **5** (150 mg, 0.29 mmol) and 2-(2,6-dioxopiperidin-3-yl)-5,6-difluoroisoindoline-1,3-dione (0.17

g, 0.58 mmol) in DMSO (5.8 ml) was added to iPr_2NEt (1.0 ml, 5.8 mmol). After stirring for 24 h at 100 °C, the reaction mixture was poured into brine and extracted with EtOAc. The combined organic layer was dried over $MgSO_4$ and concentrated *in vacuo*. The residue was purified by flash column chromatography (CH_2Cl_2/MeOH = 10:1) to afford **SJ-05** (130 mg, 57%). ^1H NMR (600 MHz, DMSO-d_6) δ 11.10 (s, 1H), 10.99 (s, 1H), 8.32–8.19 (m, 2H), 7.70 (d, J = 11.4 Hz, 1H), 7.40 (m, 2H), 7.07 (dd, J = 8.6, 2.4 Hz, 1H), 6.93 (d, J = 8.6 Hz, 1H), 6.77 (dd, J = 3.4, 2.3 Hz, 1H), 6.35 (dd, J = 3.4, 2.0 Hz, 1H), 5.10 (dd, J = 12.9, 5.4 Hz, 1H), 4.61 (d, J = 11.0 Hz, 1H), 4.45 (d, J = 10.3 Hz, 1H), 4.10 (m, 1H), 3.71–3.56 (m, 3H), 3.17 (d, J = 5.3 Hz, 3H), 2.87 (m, 3H), 2.67 (m, 3H), 2.62–2.56 (m, 1H), 2.45–2.35 (m, 4H), 2.20 (m, 2H), 2.12– 1.98 (m, 2H), 1.90–1.80 (m, 3H), 1.77–1.62 (m, 3H), 1.30–1.17 (m, 4H). HRMS (FAB+) calcd for $C_{41}H_{44}FN_{11}O_5$ $[M + H]^+$ = 790.3589, found = 790.3582.

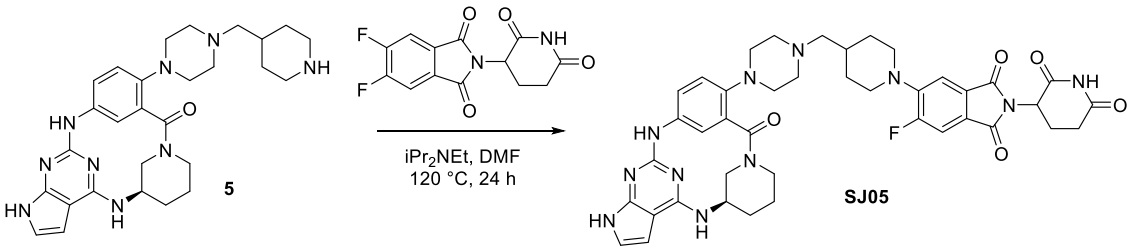

Pharmacokinetic study

In vivo pharmacokinetic studies in mice were investigated, as previously described [7]. SJ-05 (1 mg/ml) was dissolved in a mixture of DMSO, Cremophor EL, polyethylene glycol 400 and double distilled water (10/10/40/40%, v/v) for oral administration to overnight-fasted mice at 10 mg/kg. Blood samples were collected at 30, 60, 120, 240, 480, and 1440 min after oral administration. Blood samples were immediately centrifuged at 14,000 rpm for 15 min at 4°C, and supernatants (plasma) were stored at –20°C until required.

LC-MS/MS analysis and pharmacokinetic parameters

Plasma concentration levels of SJ-05 were determined by a LC-MS/MS system. The LC-MS/MS system includes an AB SCIEX Triple Quad™ 3500 (TQ3500) mass spectrometer (AB Sciex LLC, Framingham, MA, USA) connected to Agilent 1290 HPLC system (Agilent Technologies, Santa Clara, CA, USA). The chromatographic separation was performed with a Synergi^{TM} polar reverse-phase column (pore size 80 Å, particle size 4 μm, dimensions 150 × 2 mm, Phenomenex, Torrance, CA, USA). The mobile phase was a mixture of acetonitrile and 0.1% aqueous formic acid (70:30, v/v) at a flow rate of 0.2 mL/min, and the injection volume was 2 μL. In positive electrospray ionization mode by multiple reaction monitoring (MRM), the optimized MRM conditions were as follows; m/z 790.456 → 372.1 for SJ-05 and m/z 180.035→110.0 for IS. Mass data was processed using Analyst software version 1.5.2 (Applied Biosystems-SCIEX, Concord, ON, Canada). Plasma PK and standard samples were deproteinized by adding methanol including IS. The plasma calibration curve of SJ-05 in the concentration range of 50–5000 ng/mL showed good linearity with correlation coefficient (r = 0.9993 with a weighing factor of $1/x^2$). Oral pharmacokinetics parameters were calculated by non-compartmental analysis (WinNonlin® software version 8.3, Pharsight Corporation, Mountain View, CA, USA).

Statistics

All experiments requiring statistical analysis were performed at least three times with similar results. Data are expressed as the mean±standard deviation (SD). For comparisons between two groups, Student's unpaired *t*-test was employed. Comparisons among multiple groups were performed using one-way ANOVA with Bonferroni's post hoc analysis. The

Pearson correlation coefficients were calculated for continuous variables. A *p*-value less than 0.05 was considered significant. We utilized GraphPad 9.5 software for statistical analysis.

2. Supplemental Figures

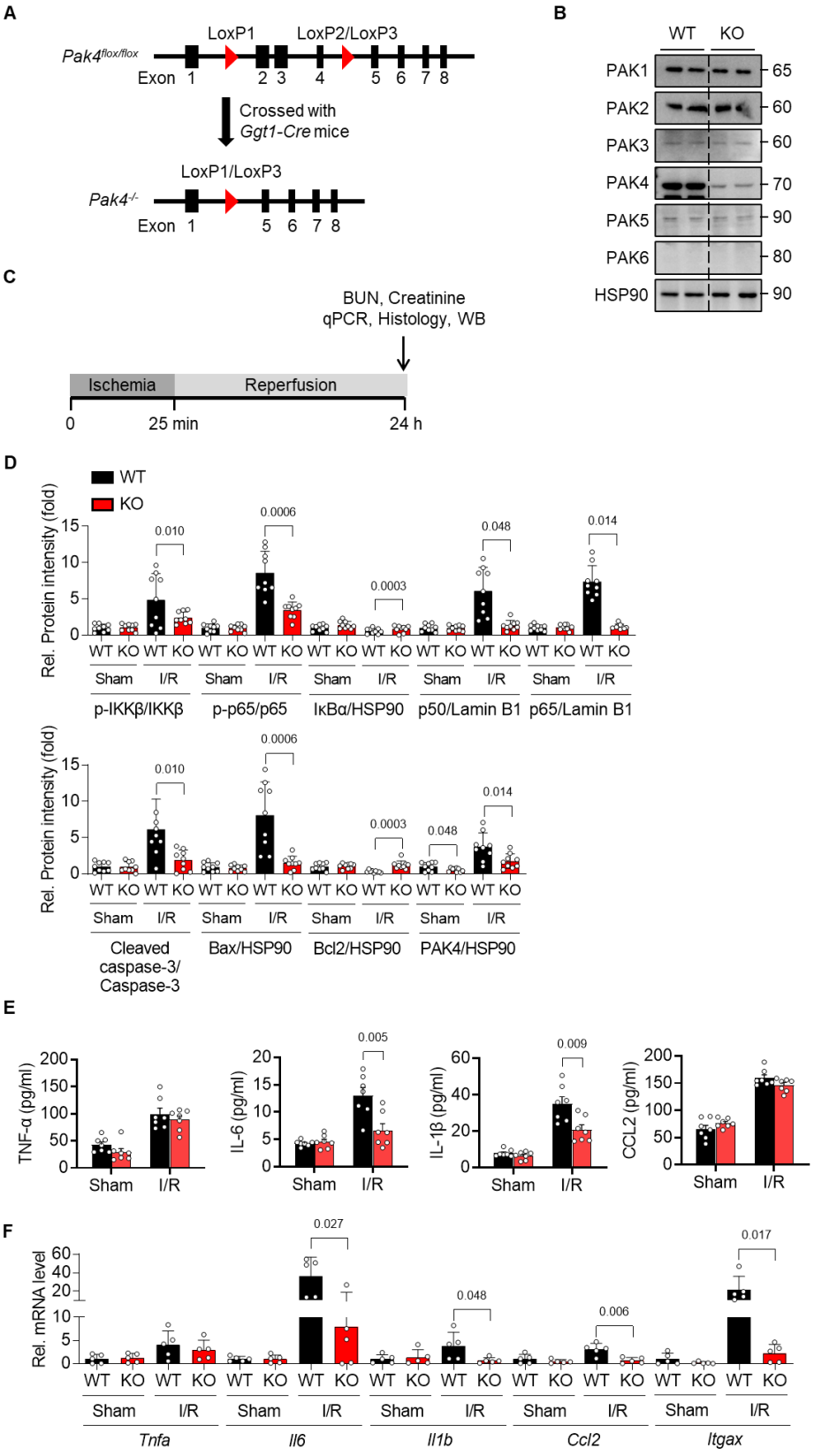

Supplemental Figure 1. Generation of renal tubule-specific *Pak4* KO mice. (A) Targeting strategy for renal tubule-specific deletion of PAK4. (B) Protein levels of PAK isotypes in kidney tissues of *Pak4* KO mice and littermate control were compared by Western blotting. (C) Schematic diagram showing experimental protocol. Mice were subjected to 25 min of ischemia followed by a 24 h reperfusion. Kidney tissues and blood samples were collected after reperfusion for each experiment. (D) The band intensity shown in Figure 2D was quantified by densitometry (n=9). (E, F) Plasma levels of cytokines and tissue levels of cytokines mRNA after I/R injury (n=5-7). Values are mean±SD.

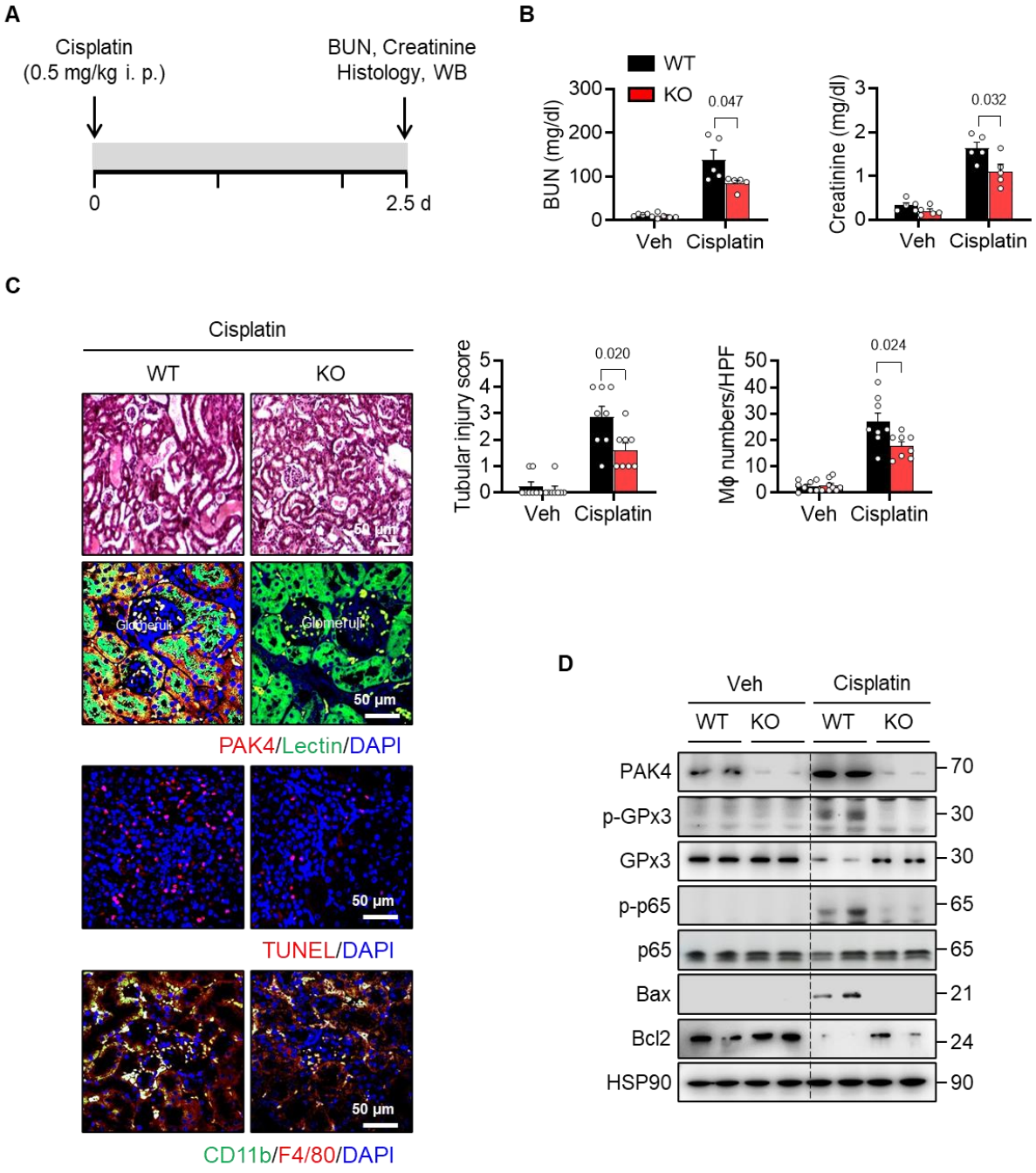

Supplemental Figure 2. Attenuation of cisplatin-induced tubular damage and inflammation in *Pak4* KO mice. (A) A schematic diagram of the experimental protocol: WT and *Pak4* KO mice were given cisplatin at 0.5 mg/kg, and after 2.5 days, kidney tissues and blood samples were collected for biochemical, histological, and Western blot analyses. (B) Plasma levels of blood urea nitrogen (BUN) and creatinine (n=5). (C) Microscopic pictures of kidney sections and quantification of tubular injury score (from H&E) and macrophage (MΦ) numbers (from F4/80) in kidney tissues (n=8). (D) Western blot analysis of oxidative stress, apoptosis signaling and inflammation marker molecules in kidney tissues. Values are mean±SD. HPF, high power field.

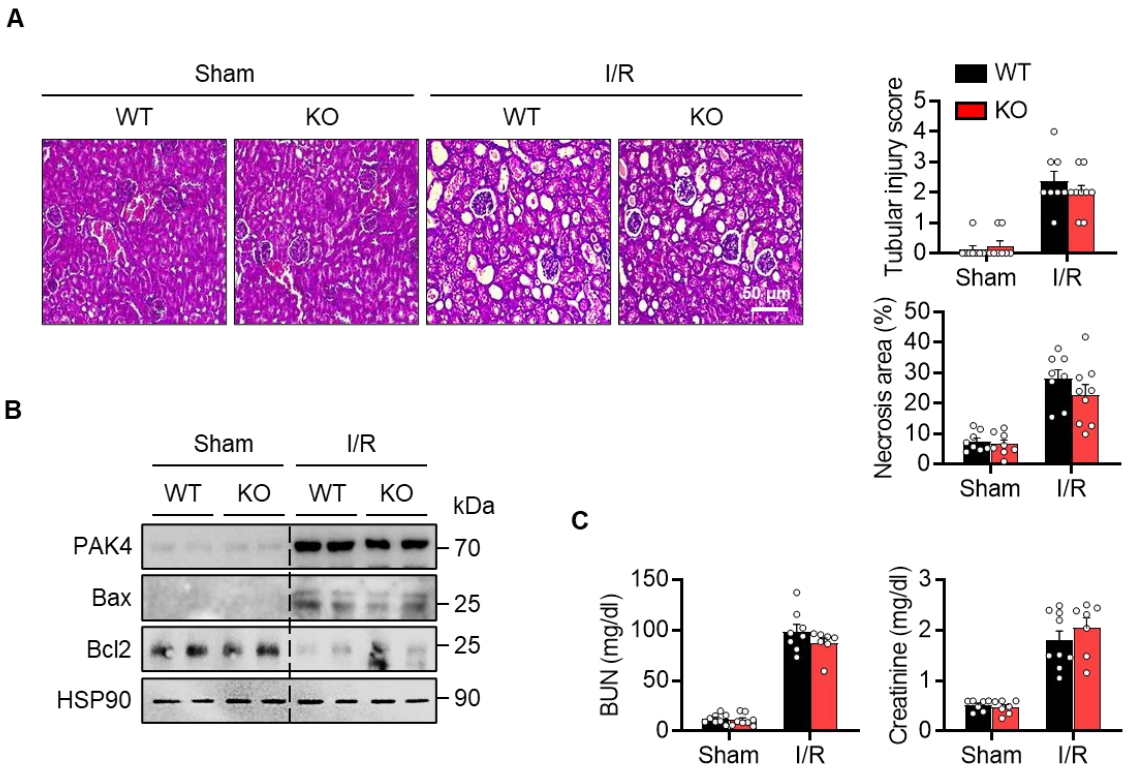

Supplemental Figure 3. No effects of myeloid PAK4 deficiency on renal I/R injury. (A) Myeloid *Pak4* KO and littermate control mice were subjected to renal I/R injury. H&E staining of kidney sections and the measurement of tubular injury score and necrosis area in H&E sections (*n*=8 or 9). (B) Western blotting of PAK4 and apoptosis-related proteins. (C) Plasma levels of BUN and creatinine (*n*=7-9). Values are mean±SD.

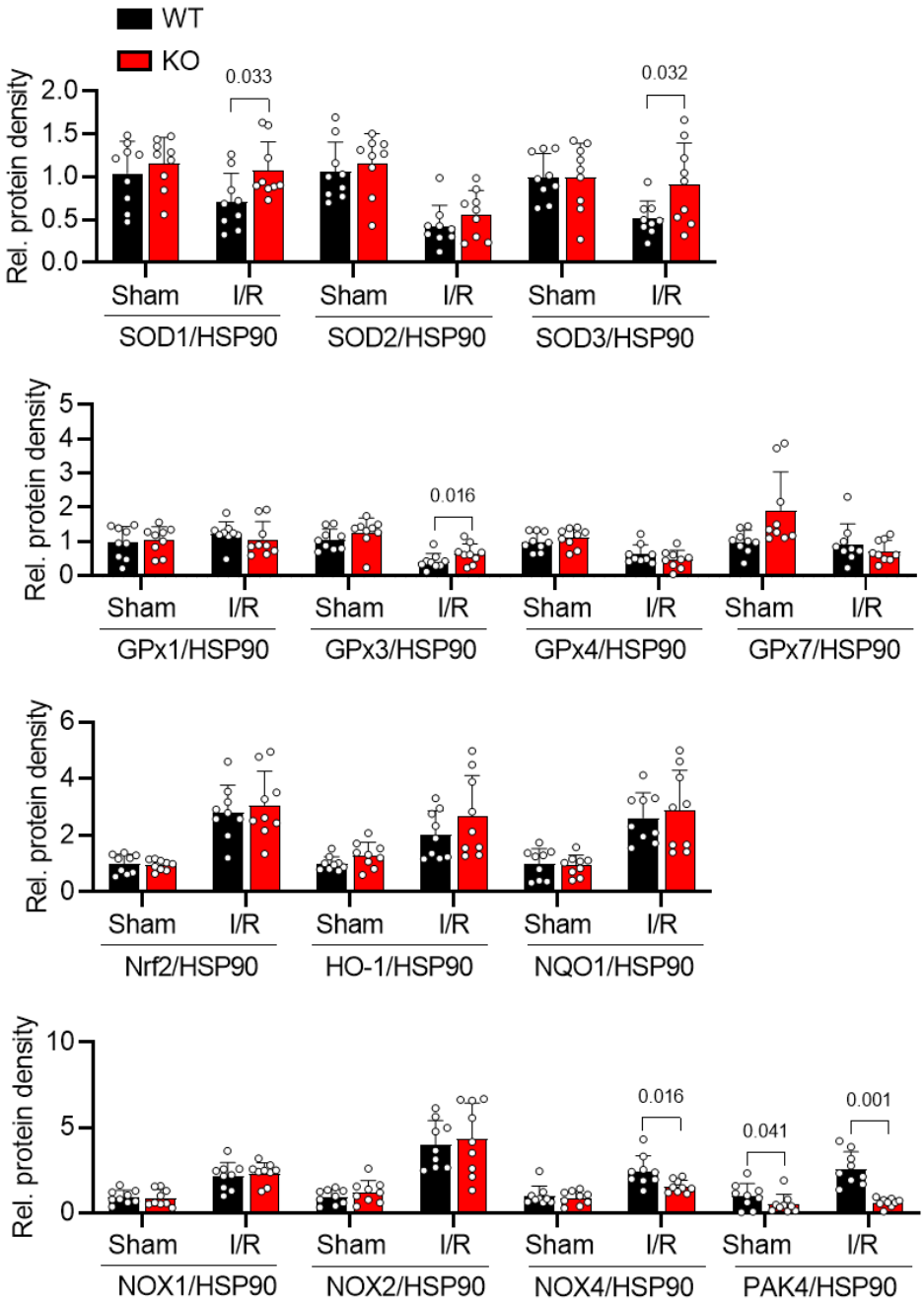

Supplemental Figure 4. Protein quantification. The band intensity shown in Figure 3C was quantified by densitometry (*n*=9). Values are mean±SD.

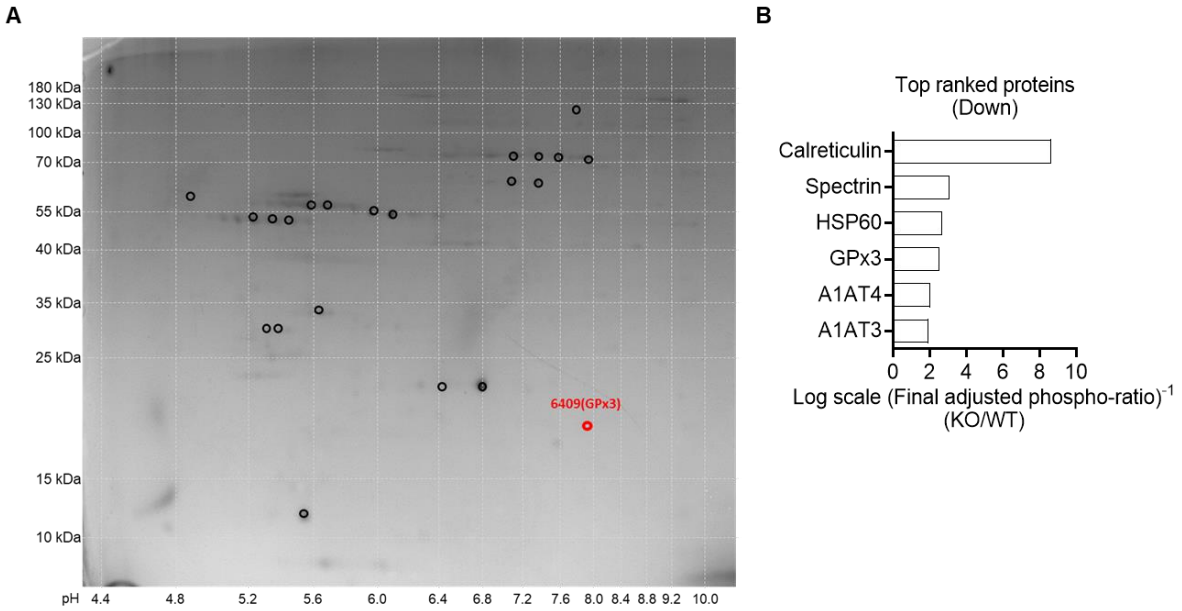

Supplemental Figure 5. Phosphoproteomic analysis of kidney tissues. (A) A representative phosphoimage of two-dimensional polyacrylamide gel electrophoresis. The proteins that showed a visible difference in phosphorylation levels are indicated by circles and labeled with serial numbers. Spot no. 6409 (shown as red circle) corresponds to glutathione peroxidase 3 (GPx3). (B) Whole cell lysates were subjected to LC-MS/MS phospho-tryptic peptide identification and quantification. The top ranked phospho-proteins are presented.

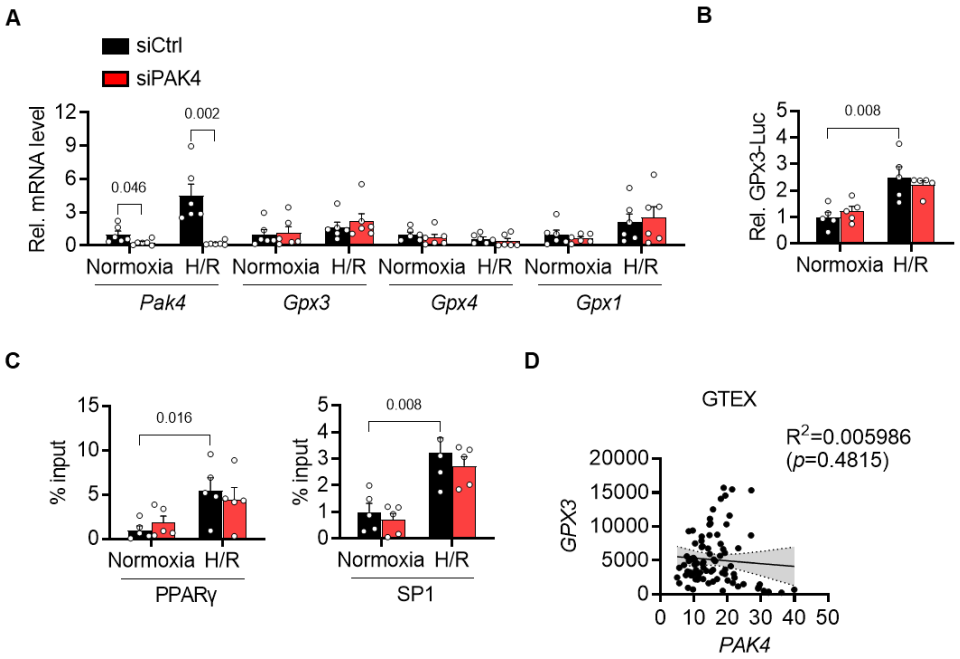

Supplemental Figure 6. The effects of PAK4 on glutathione peroxidase 3 (GPx3) transcription. (A-C) HK-2 cells were transfected with scrambled siRNA (siCtrl) or siRNA against PAK4 (siPAK4) and then exposed to H/R. mRNA levels of *Pak4* and *Gpx* isotypes (A, *n*=6), GPx3-luciferase activities (B, *n*=5), and ChIP-qPCR assay (C, *n*=5) were assessed. (D) Genotype tissue expression (GTEx) analysis of human kidney tissues (*n*=85). Coefficient of determination (R^2) between *PAK4* and *GPX3* were calculated. Values are mean±SD.

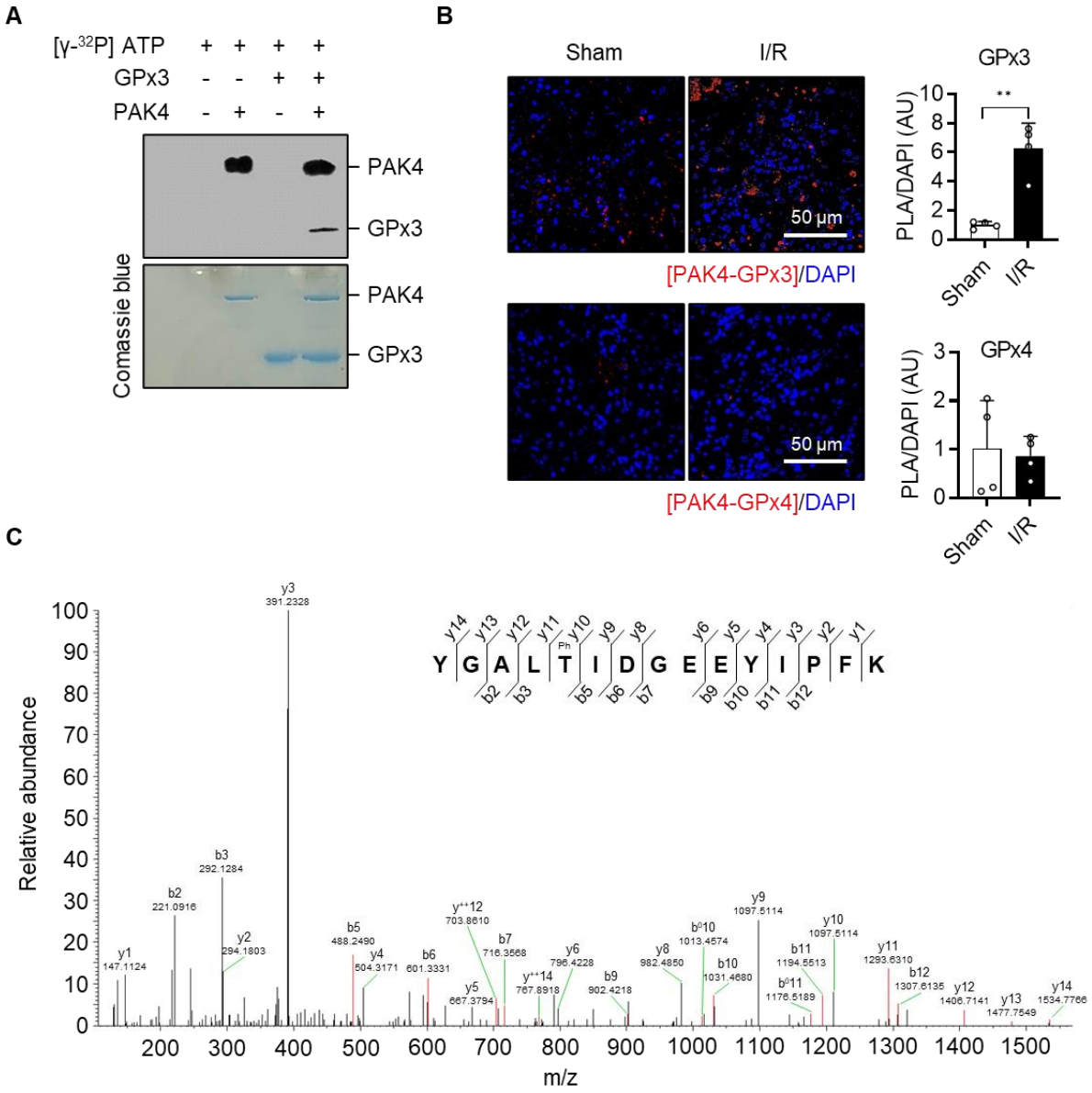

Supplemental Figure 7. Binding and phosphorylation of glutathione peroxidase 3 (GPx3) by PAK4. (A) *In vitro* phosphorylation of GPx3 by PAK4. An incubation of recombinant GPx3 with [γ-^{32}P]ATP with or without PAK4, followed by autoradiography and Coomassie brilliant blue staining. (B) Following 24 h-reperfusion, PAK4 binding to either GPx4 or GPx3 was analyzed by proximity ligation assay (PLA, *n*=4). (C) HK-2 cells were transfected with PAK4 and then exposed to H/R, after which phosphorylation of GPx3 was determined in PAK4 immunoprecipitates using LC-MS/MS analysis after in-gel digestion. MS/MS spectra revealing the phosphorylation of GPx3 at T47 was observed.

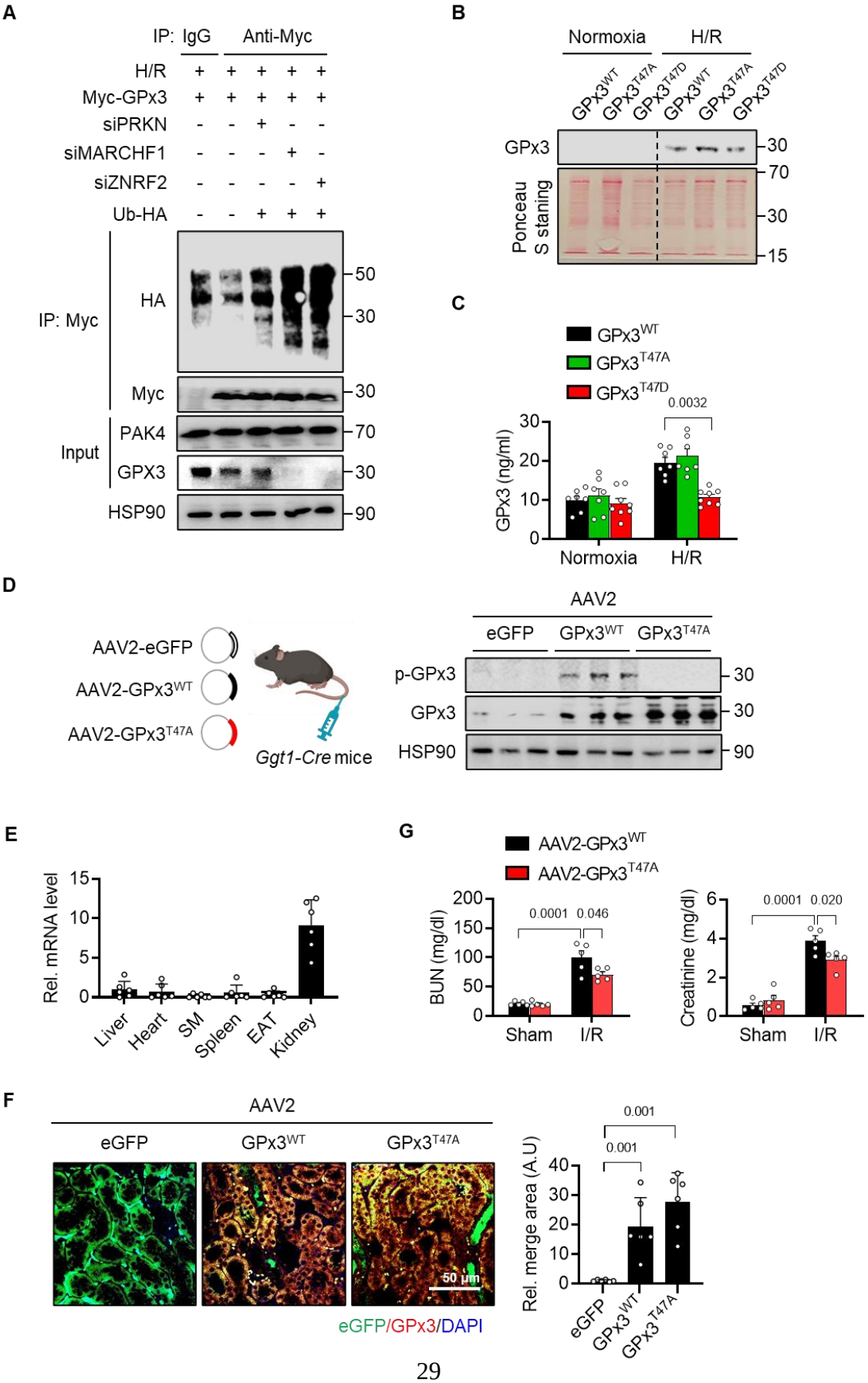
A
IP: IgG
Anti-Myc
H/R
Myc-GPx3
siPRKN
siMARCHF1
siZNRF2
Ub-HA
IP: Myc
HA
Myc
Input
PAK4
GPX3
HSP90
50
30
30
70
30
90
B
Normoxia
H/R
GPx3WT
GPx3T47A
GPx3T47D
GPx3
Ponceau S staning
30
70
30
15
C
GPx3WT
GPx3T47A
GPx3T47D
0.0032
GPx3 (ng/ml)
Normoxia
H/R
D
AAV2-eGFP
AAV2-GPx3WT
AAV2-GPx3T47A
Ggt1-Cre mice
AAV2
eGFP
GPx3WT
GPx3T47A
p-GPx3
GPx3
HSP90
30
30
90
E
Rel. mRNA level
Liver
Heart
SM
Spleen
EAT
Kidney
G
AAV2-GPx3WT
AAV2-GPx3T47A
BUN (mg/dl)
0.0001
0.046
Sham
I/R
Creatinine (mg/dl)
0.0001
0.020
Sham
I/R
F
AAV2
eGFP
GPx3WT
GPx3T47A
50 μm
eGFP/GPx3/DAPI
Rel. merge area (A.U)
0.001
0.001
eGFP
GPx3WT
GPx3T47A

Supplemental Figure 8. Destabilization of glutathione peroxidase 3 (GPx3) by PAK4. (A) HK-2 cells transfected with either control siRNA or siRNA targeting PRKN, MARCHF1 and ZNRF2 were exposed to H/R for 12 h. Cell lysates were immunoprecipitated with anti-GPx3 antibody followed by immunoblotting with anti-ubiquitin (Ub) antibody. (B, C) After transfecting HK-2 cells with phospho-deficient GPx3 ($GPx3^{T47A}$) or phospho-mimetic GPx3 ($GPx3^{T47D}$), the cells were exposed to H/R for 12 h, and protein level of GPx3 in the cells (B) and secretion of GPx3 into the culture media (C, *n*=7 or 8) were analyzed. (D-G) Eight-week-old male *Ggt1-Cre* KO mice were injected intravenously with AAV2 expressing eGFP (AAV2-eGFP), GPx3 (AAV2-$GPx3^{WT}$), or $GPx3^{T47A}$ (AAV2-$GPx3^{T47A}$). Protein levels of GPx3 in kidney tissues (D), mRNA levels of *Gpx3* in various organs (E), immunofluorescence staining of GPx3 in kidney tissues (F), and plasma levels of BUN and creatinine (G, *n*=5) were determined. Values are mean±SD. PRKN, Parkin RBR E3 ubiquitin protein ligase; MARCHF1, membrane associated ring-CH-type finger 1; ZNRF2, Zinc and ring finger 2.

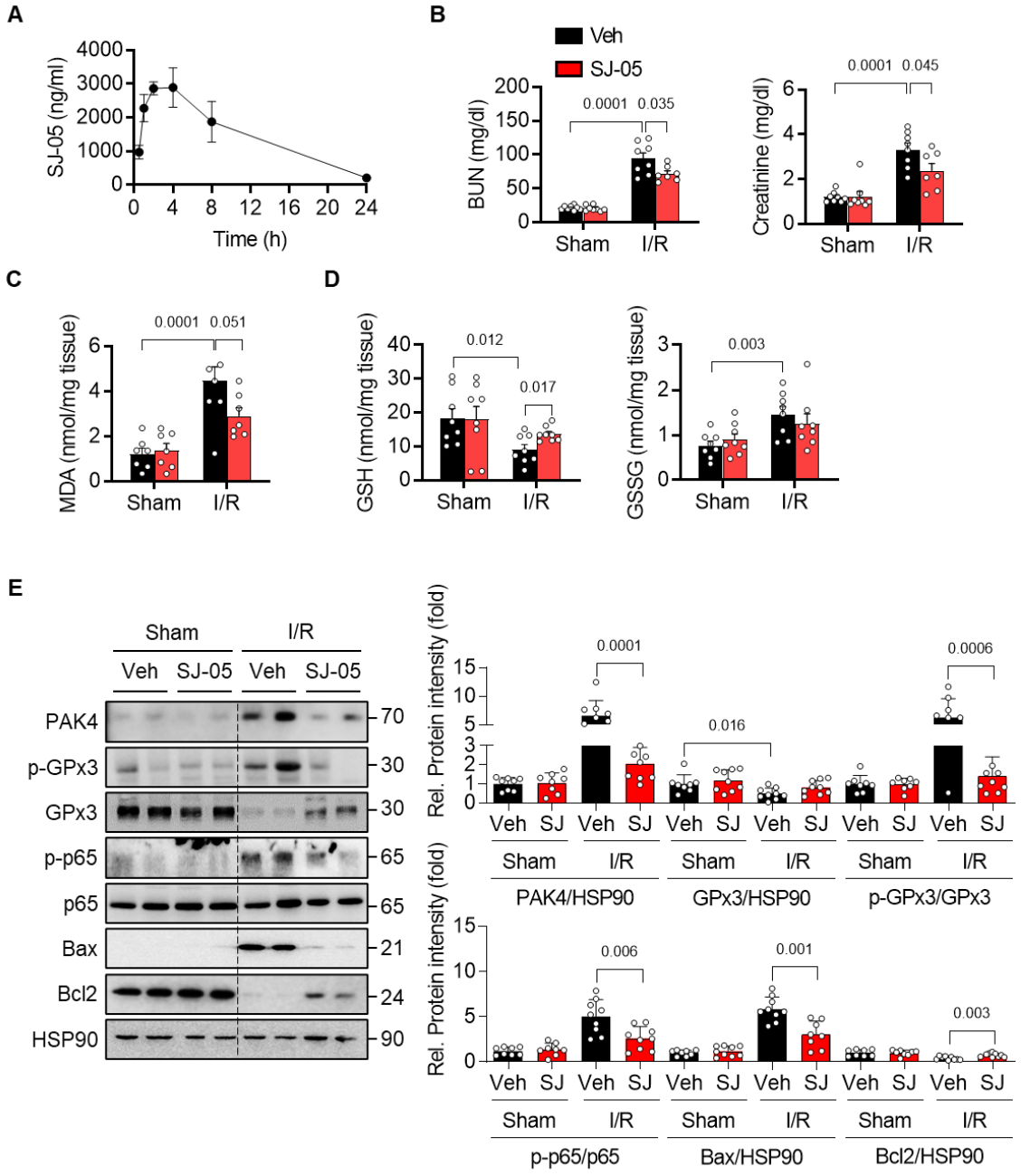

Supplemental Figure 9. Attenuation of renal I/R injury by PAK4 PROTAC SJ-05. (A) In vivo pharmacokinetics of SJ-05 in mice. Average plasma drug concentration-time profile of SJ-05 was obtained after oral administration to mice at a dose of 10 mg/kg (*n*=3). (B-E) All experimental procedures were the same as those described in Figure 7B's legend. (B) Plasma levels of BUN and creatinine (*n*=7 or 8). (C, D) Tissue levels of MDA, GSH and GSSG (*n*=8-10). (E) Western blotting of PAK4 and inflammation- and apoptosis-related proteins (*n*=8 or 9). Values are mean±SD. Veh, vehicle.

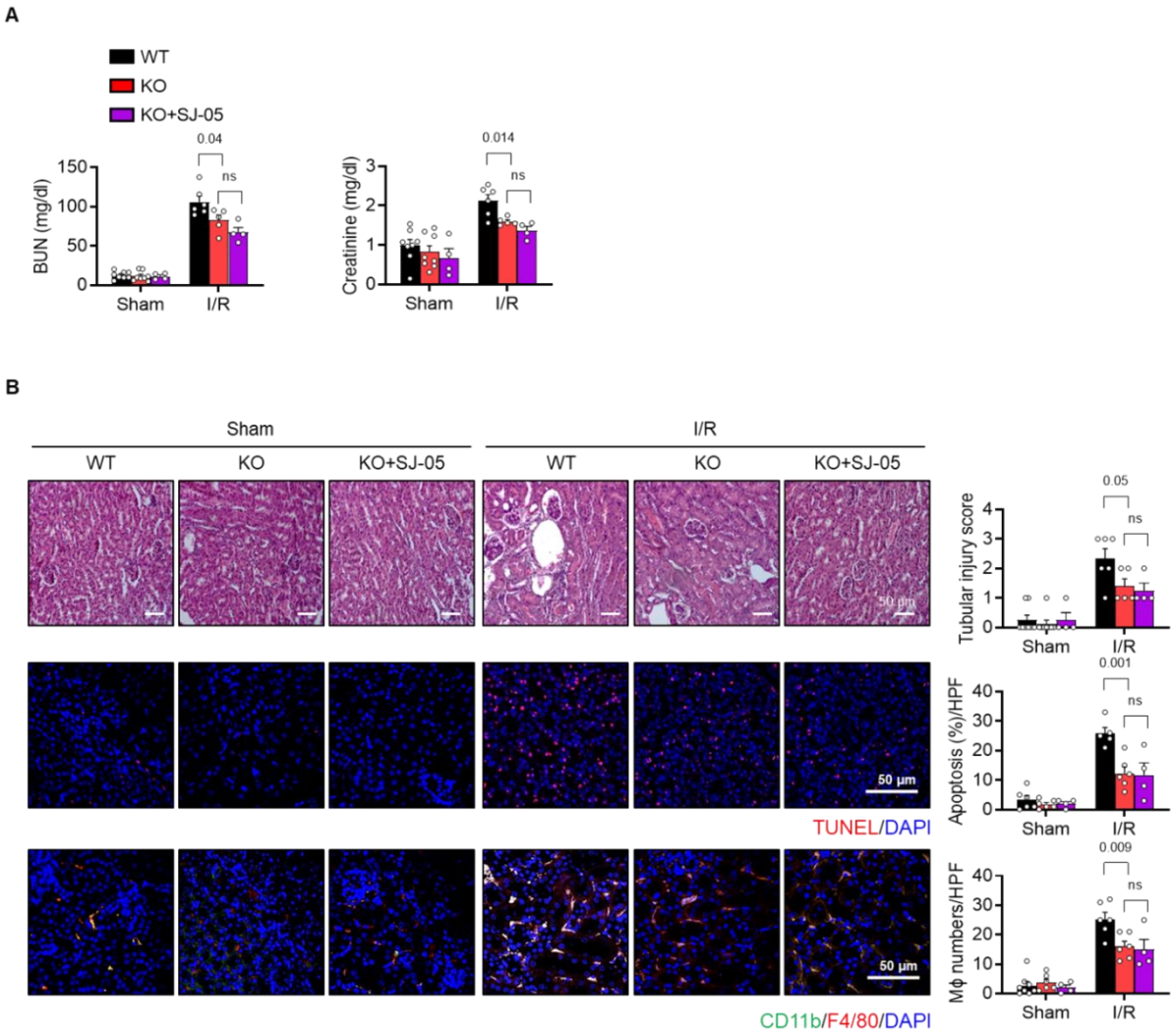

Supplemental Figure 10. On-target effects of SJ-05 treatment. The experimental conditions were identical to those described in Figure 7B, with the addition of *Pak4* KO mice. (A) Plasma levels of BUN and creatinine (*n*=4-9). (B) Microscopic images of kidney sections, along with quantification of tubular injury score (from H&E), apoptosis (from TUNEL), and macrophage numbers (from F4/80) in kidney tissues (*n*=4-9). Values are mean±SD.

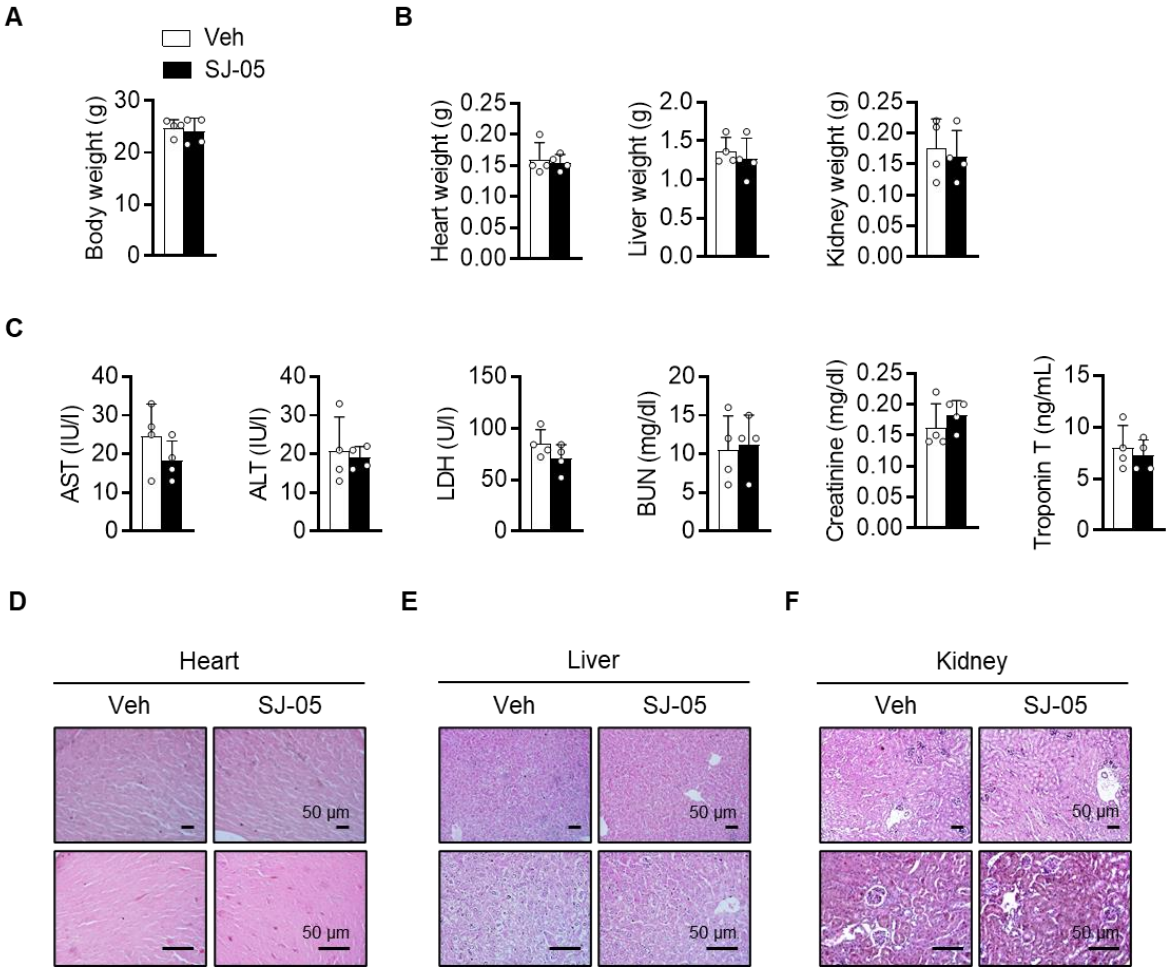

Supplemental Figure 11. No potential acute side effects of SJ-05. SJ-05 (50 mg/kg body weight) was orally administered for two times as depicted in Figure 7B. Twenty-four hours after the last dose, body weights (A, *n*=4), the weights of liver, heart, and kidney (B, *n*=4) and serum levels of AST, ALT, LDH, BUN, creatinine, and troponin T (C, *n*=4) were determined. (D-F) Tissue sections of heart (D), liver (E), and kidney (F) were prepared and stained by H&E. Values are mean ± SD.

3. Supplemental Tables

Supplemental Table 1. Calculated stoichiometry of phosphorylation based on label-free LC/MS data.

Protein	Modification site	Spectra count of peptide			Stoichiometry (%)
		Non-modified	Phosphorylated	Total #	
GPx3	T47	7732	4489	12221	0.3673

Supplemental Table 2. Pharmacokinetic parameters of SJ-05 following oral doses of 10 mg/kg in mice. The data are expressed as the mean ± SD (*n*=3), except for T_{max}, which is shown as median values along with their range.

Parameters	SJ-05
T_{max} (min)	200 ± 69 [120-240]
C_{max} (μg/ml)	3.16 ± 0.11
$T_{1/2}$ (min)	311 ± 34
AUC_{last} (μg·min/ml)	1847 ± 394
AUC_{inf} (μg·min/ml)	1942 ± 429
MRT (min)	526 ± 50

T_{max}, time to peak drug concentration; C_{max}, maximum concentration; AUC_{last}, area under the curve to the last measurable concentration, AUC_{inf}, area under the curve from time zero to infinity, MRT, mean residence time.

Supplemental Table 3. Clinical factors and graft outcome indicators after transplantation

Clinical details	Recipients (*n*=15)
Age	57.75 ± 7.65
Gender (M/F)	9/3
Cold ischemia time (min)	85.58 ± 76.75
Warm ischemia time (min)	42.08 ± 6.73
Kidney weight	186.98 ± 43.33
Pre-operational-eGFR (ml/min/1.7)	9.15± 3.89
No. of rejection episode	1

Values are mean ± SD.

†Positive crossmatch resulting from non-HLA, autoreactive IgM antibodies.

‡Delayed graft function is defined as the requirement for dialysis in the first week after transplantation.

Supplemental Table 4. Antibodies used for Western blotting, immunofluorescence and immunohistochemical analyses

Antibodies	Resource	Identifier	Dilution
PAK4	Cell Signaling Technology	#G222	1:2000
p-PAK4 (S474)	Cell Signaling Technology	#3241	1:2000
PAK1	Cell Signaling Technology	#2602	1:2000
PAK2	Cell Signaling Technology	#2608	1:2000
PAK3	Cell Signaling Technology	#2609	1:2000
PAK5	Cell Signaling Technology	#62234	1:2000
PAK6	Santa Cruz Biochemicals	#sc-393075	1:2000
Ub-HA	Abcam	#ab236632	1:2000
p-Thr	Millipore	#AB1607	1:1000
p-Ser	Millipore	#AB1603	1:1000
Total OXPHOS	Abcam	#ab110413	1:1000
HIF1α	Cell Signaling Technology	#36169	1:2000
HIF1β	Cell Signaling Technology	#5537	1:2000
HIF2α	Cell Signaling Technology	#59973	1:2000
p-IKKβ1	Cell Signaling Technology	#2078	1:2000
IKKβ1	Cell Signaling Technology	#8943	1:2000
p-p65	Cell Signaling Technology	#3033	1:2000
p65	Cell Signaling Technology	#8242	1:2000
p50	Cell Signaling Technology	#3035	1:2000
IκBα	Cell Signaling Technology	#9242	1:2000
Bax	Cell Signaling Technology	#5023	1:2000
Bcl2	Cell Signaling Technology	#3498	1:2000
Cleaved caspase 3	Cell Signaling Technology	#9664	1:2000
Caspase 3	Cell Signaling Technology	#14220	1:2000
Calreticulin	Cell Signaling Technology	#92635	1:2000
Spectrin	Abcam	#ab154811	1:2000
HSP60	Cell Signaling Technology	#4870	1:2000
Lotus lectin	CD bio	#X23-02-ZQ878	1:2000
Nephrin	Abcam	#ab216341	1:2000
F4/80	Santa Cruz Biochemicals	Sc-377009	1:2000
Lamin b1	Cell Signaling Technology	#12586	1:2000
GPx1	Cell Signaling Technology	#3286	1:2000
GPx3	Abcam	#ab256470	1:2000
GPx7	Abcam	#ab96257	1:2000
HO-1	Cell Signaling Technology	#26416	1:2000
NQO1	Cell Signaling Technology	#62262	1:2000
NOX1	Cell Signaling Technology	#ab131088	1:2000
NOX2	Cell Signaling Technology	#ab129068	1:2000

NOX4	Abcam	#ab154244	1:2000
SOD1	Cell Signaling Technology	#65778	1:2000
SOD2	Cell Signaling Technology	#13141	1:2000
SOD3	Abcam	#ab80946	1:2000
Nrf2	Cell Signaling Technology	#12721	1:2000
NCoR1	Cell Signaling Technology	#5948	1:2000
PPARα	Abcam	#ab126285	1:2000
HSP90	Enzo Life Sciences	#ADI-SPA-836-F	1:2000
PARKIN	Abcam	#ab77924	1:2000
MARCHF1	Abcam	#ab251706	1:2000
ZNRF2	Abcam	#ab156011	1:2000
Myc	Cell Signaling Technology	#9402	1:1000
FLAG	Cell Signaling Technology	#14793	1:1000
F4/80	Abcam	#ab16911	1:100
Podocin	Boster	#PA1322-1	1:100
Aquaporin-4	Abcam	#ab259318	1:100
eGFP	Thermo Fisher Scientific	#F56-6A1.2.3	1:100
Plin2	Abcam	#ab108323	1:100
PAK4	Santa Cruz Biochemicals	Sc-390507	1:100
Lotus Tetragonolobus (Asparagus Pea) Lectin	Thermo Fisher Scientific	#L32480	1:100
Alexa Fluor 488-conjugated goat anti-mouse IgG1	Thermo Fisher Scientific	#11001	1:100
Alexa Fluor 594-conjugated goat anti-rabbit IgM	Thermo Fisher Scientific	#11012	1:100

Supplemental Table 5. Sequences and accession numbers for primers (forward, FOR; reverse, REV) used in qPCR

Gene	Forward (5′ → 3′)	Reverse (5′ → 3′)	Access No.
Pak4	GCTCCCCTTTGAAGATGTCA	GACCCACAAGGACTCAAGGA	NM_027470.3
PAK 4	GGACATCAAGAGCGACTCGAT	CGACCAGCGACTTCCTTCG	NM_001014834
Hif1b	TTCCCCAGAATCCCTTTGCC	TGGTTCATCTTGTCTCTCCGAC	NM_172309
Gpx1	CCACCGTGTATGCCTTCTCC	AGAGAGACGCGACATTCTCAAT	NM_008160
Gpx3	CCTTTTAAGCAGTATGCAGGCA	CAAGCCAAATGGCCCAAGTT	NM_008161
Tnfa	GCGGCCACAGAAAACACTC	CTCCCAATGGTCAAGGCATC	NM_001001495
Il6	TGGGGCTCTTCAAAAGCTCC	AGGAACTATCACCGGATCTTCAA	NM_028430
Il1	GAAATGCCACCTTTTGACAGTG	TGGATGCTCTCATCAGGACAG	NM_008361
Ccl2	TTCTTCGATTTGGGTCTCCTTG	GTGCAGCTCTTGTCGGTGAA	NM_001013412
Itgax	CTGGATAGCCTTTCTTCTGCTG	GCACACTGTGTCCGAACTCA	NM_021334
Chip GPx3	CAGCTAGTCACATGCCTCCA	TCAGCAGGTAAAAGCCCTCA	

4. Supplemental References

1. Yoon HY, Kang NI, Lee HK, Jang KY, Park JW, Park BH. Sulforaphane protects kidneys against ischemia-reperfusion injury through induction of the Nrf2-dependent phase 2 enzyme. *Biochem Pharmacol*. 2008;75(11):2214-2223. doi:10.1016/j.bcp.2008.02.029

2. Cheng YT, Tu YC, Chou YH, Lai CF. Protocol for renal ischemia-reperfusion injury by flank incisions in mice. *STAR Protoc*. 2022;3(4):101678. doi:10.1016/j.xpro.2022.101678

3. Shi MY, Yu HC, Han CY, et al. p21-activated kinase 4 suppresses fatty acid beta-oxidation and ketogenesis by phosphorylating NCoR1. *Nat Commun*. 2023;14(1):4987. doi:10.1038/s41467-023-40597-z

4. Baskaran Y, Ang KC, Anekal PV, et al. An in cellulo-derived structure of PAK4 in complex with its inhibitor Inka1. *Nat Commun*. 2015;6:8681. doi:10.1038/ncomms9681

5. Khramushin A, Marcu O, Alam N, et al. Modeling beta-sheet peptide-protein interactions: Rosetta FlexPepDock in CAPRI rounds 38-45. *Proteins*. 2020;88(8):1037-1049. doi:10.1002/prot.25871

6. London N, Raveh B, Cohen E, Fathi G, Schueler-Furman O. Rosetta FlexPepDock web server--high resolution modeling of peptide-protein interactions. *Nucleic Acids Res*. 2011;39(Web Server issue):W249-253. doi:10.1093/nar/gkr431

7. Park SY, Gurung R, Hwang JH, et al. Development of KEAP1-targeting PROTAC and its antioxidant properties: In vitro and in vivo. *Redox Biol*. 2023;64:102783. doi:10.1016/j.redox.2023.102783